

PRODUCTION OF TEV GAMMA-RADIATION IN THE VICINITY OF THE SUPERMASSIVE BLACK HOLE IN THE GIANT RADIOGALAXY M87

A. NERONOV

INTEGRAL Science Data Center,
16 ch. d'Ecogia, CH-1290, Versoix, Switzerland
and
Geneva Observatory, University of Geneva
51 ch. des Maillettes, CH-1290 Sauverny, Switzerland

AND

FELIX A. AHARONIAN

Dublin Institute for Advanced Studies, 5 Merrion Square, Dublin 2, Ireland
and
Max Planck Institut für Kernphysik, Saupfercheckweg 1, 69117 Heidelberg, Germany
Draft version October 27, 2018

ABSTRACT

Although the giant radiogalaxy M 87 harbors many distinct regions of broad-band nonthermal emission, the recently reported fast variability of TeV γ -rays from M 87 on a timescale of days strongly constrains the range of speculations concerning the possible sites and scenarios of particle acceleration responsible for the observed TeV emission. A natural production site of this radiation is the immediate vicinity of the central supermassive mass black hole (BH). Because of the low bolometric luminosity, the nucleus of M 87 can be effectively transparent for γ -rays up to energy of 10 TeV, which makes this source an ideal laboratory for study of particle acceleration processes close to the BH event horizon. We critically analyse different possible radiation mechanisms in this region, and argue that the observed very high-energy γ -ray emission can be explained by the inverse Compton emission of ultrarelativistic electron-positron pairs produced through the development of an electromagnetic cascade in the BH magnetosphere. We demonstrate, through detailed numerical calculations of acceleration and radiation of electrons in the magnetospheric vacuum gap, that this “pulsar magnetosphere like” scenario can satisfactorily explain the main properties of TeV gamma-ray emission of M 87.

Subject headings: gamma rays: theory — black hole physics — galaxies: active — galaxies: individual (M 87)

1. INTRODUCTION

M 87, a nearby giant radio galaxy, located at a distance of $d \simeq 16$ Mpc (Tonry 1991), hosts one of the most massive ($M \simeq 3 \times 10^9 M_{\odot}$) black holes (BH) in the nearby Universe (Marconi et al. 1997). M 87 contains a famous kpc-scale jet the high-resolution images of which detected at radio, optical and X-ray wavelengths show several prominent structures. Nonthermal processes play important, if not the dominant, role across the entire jet. The apparent synchrotron origin of the detected nonthermal emission, which extends from radio to X-ray bands, implies effective acceleration of electrons to multi-TeV energies. One may expect that protons and nuclei, which do not suffer radiative losses, are accelerated to much higher energies. Both the inner (sub-parsec) and large (kpc) scale parts of the jet of M 87 are possible sites of acceleration of protons to extremely high energies ($E \sim 10^{20}$ eV). Therefore production of gamma-rays in different segments of the jet due to electromagnetic or hadronic processes is not only possible, but, in fact, unavoidable. The jet of M 87 is observed at large angle, $\sim 20^\circ$ (Biretta et al. 1999). Therefore, unlike blazars, we do not expect a strong Doppler boosting of the γ -ray flux. On the other hand, the nearby location of M 87 compensates this disadvantage (compared to blazars) and makes

several prominent knots and hot spots of the jet as potentially detectable TeV γ -ray emitters.

In this regard, the discovery of a TeV γ -ray signal from M 87 by the HEGRA array of Cherenkov telescopes (Aharonian et al. 2003) and its confirmation by the HESS array of telescopes (Aharonian et al. 2006), was not a big surprise, especially given the rather modest apparent TeV γ -ray luminosity (few times 10^{40} erg/cm²s). Several electronic and hadronic models have been suggested for explanation of TeV γ -ray emission of M87. The suggested sites of TeV γ -ray production range from large scale structures of the kpc jet (Stawarz et al. 2005) to a compact peculiar hot spot (the so-called *HST*-1 knot) at a distance 100 pc along the jet (Stawarz et al. 2006) and inner (sub-parsec) parts of the jet (Georganopoulos et al. 2005; Reimer et al. 2005).

While gamma-ray observations cannot provide images with an adequate resolution which would allow localisation of sites of γ -ray production, the variability studies can discard or effectively constrain the suggested models.

The continuous monitoring of M 87 with the HESS telescope array during the period 2003-2006 not only revealed statistically significant fluctuations of the TeV flux on a yearly basis, but, more excitingly, an evidence of fast variability on timescales of $\Delta t \sim 2$ days was found in the 2005 dataset (Aharonian et al. 2006). This requires a very compact region with a characteristic linear

size $R \leq \Delta t \delta_j \simeq 5 \times 10^{15} \delta_j$ cm, where δ_j is the Doppler factor of the relativistically moving source (throughout the paper we will use the system of units in which the speed of light $c = 1$). Note that since the mass of the BH in M 87 is well established (Marconi et al. 1997), the Schwarzschild radius is estimated quite accurately $R_{\text{Schw}} = 2GM \simeq 10^{15} [M/3 \times 10^9 M_\odot]$ cm (G is the gravitational constant). The expected minimal variability time scale (light crossing time of the black hole) for a non-rotating BH is $T_{\text{ls}} = 2R_{\text{Schw}}/c \simeq 6 \times 10^4 s \simeq 1$ day, while it is two times less for the maximally rotating Kerr BH. The observed variability time scale of TeV emission of ~ 2 days indicates that the emission originates within the last stable orbit of rotation around the black hole, unless the radiation is produced in relativistically moving outflow with a Doppler factor ≥ 10 . Although there are sound arguments against M 87 being a blazar (Fabian 2006), one cannot in principle exclude that at the base of its formation (close to the BH), where γ -rays are produced, the jet is pointed to us, and only later, it deviates from our line of sight. In this regard, both leptonic (Georganopoulos et al. 2005) and hadronic (Reimer et al. 2005) models suggested for TeV radiation of M 87 cannot be discarded. Note however, that both models predict rather steep energy spectra contrary to the observed hard γ -ray spectrum extending to $E \geq 10$ TeV (Aharonian et al. 2006). Whether these models are flexible enough to reproduce the observed TeV γ -ray spectrum by tuning the relevant model parameters and introducing additional assumptions, should show further detailed theoretical studies.

Finally, one should mention that formally one may assume that γ -rays are produced in a compact region far from the central engine. In this regard, the famous *HST*-1 knot has certain attractive features which make this compact structure a potential site of particle acceleration and γ -ray production (Stawarz et al. 2006). Although the favored size of this structure is in the range between 0.1 and 1 pc, and thus contradicts the observed TeV γ -ray variability, the lack of robust lower limits on the size of *HST*-1 leaves the γ -ray production in this peculiar knot as a possible option. Nevertheless one should note that the location of *HST*-1 at a distance of 100 pc from the central BH requires (almost) unrealistically tight collimation of the jet.

In this paper we assume that the TeV γ -ray production takes place close to the event horizon of the central supermassive BH, and show that the acceleration of electrons in a vacuum gap in BH magnetosphere can explain the general characteristics of the TeV γ -ray emission observed from M87.

Such mechanism of γ -ray emission from the vicinity of a black hole is a close analog of the mechanism of pulsed γ -ray emission from the vicinity of neutron stars in pulsars. The similarity between the electrodynamics of the pulsar and black hole magnetospheres was discussed in the seminal paper of Blandford & Znajek (1977) in the context of pair production and energy transfer of rotational energy of a black hole through the Poynting flux. The mechanisms of emission of high energy γ -rays from the direct vicinity of black holes by electrons and protons accelerated in the electric field of vacuum gaps were discussed by Blandford & Znajek (1977) (electron curvature

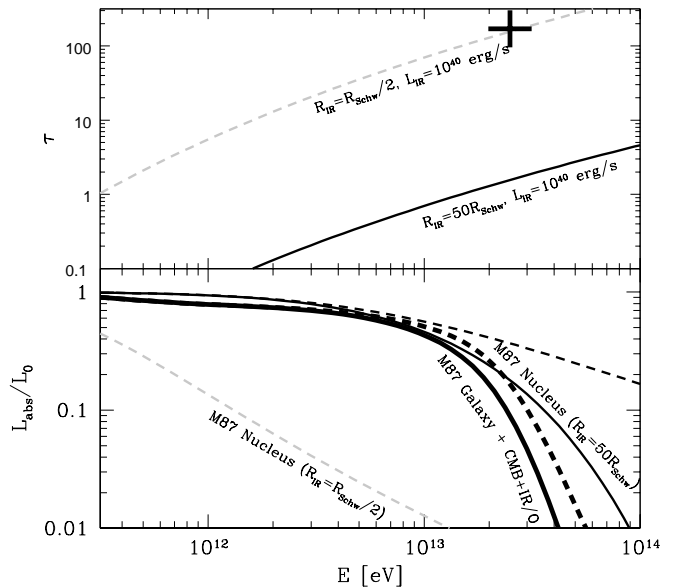


FIG. 1.— Top panel: optical depth for γ -rays produced in the vicinity of the black hole in the cases of the infrared source of size $50R_{\text{Schw}}$ (black solid curve) and $R_{\text{Schw}}/2$ (grey dashed curve). The estimate of (Cheung et al. 2007) is shown by a cross. The spectrum of the infrared background in the source is the one shown by red dashed curve in Fig. 8). Bottom panel: attenuation of γ -rays in M 87 due to photon-photon pair production. The internal absorption (thin solid curve) is dominated by interactions with the infrared radiation of the compact source in the core of M 87. The external absorption due to the interaction with the diffuse radiation fields within the elliptical galaxy M 87, the 2.7 K CMBR and the diffuse extragalactic infrared background photons leads to a further suppression of the γ -ray flux, shown by thick solid curve. Attenuation in the case when the γ -ray emission is distributed throughout the infrared source is shown by thin (intrinsic absorption in the source) and thick (modification during the propagation through the galactic and extragalactic background light) dashed curves. Dashed grey curve shows the absorption of the γ -ray flux in the case of a “maximally compact” infrared source of the size $R_{\text{IR}} = R_{\text{Schw}}/2$ (see text).

radiation), Beskin et al. (1992) (inverse Compton scattering by electrons) and Levinson (2000) (proton curvature radiation).

2. INTERNAL ABSORPTION OF γ -RAYS

The observed infrared luminosity of the nucleus of M 87, $\nu L_\nu \sim 10^{40 \pm 41}$ erg/s (Perlman et al. 2001; Whyson & Antonucci 2004) is 6.5 orders of magnitude lower than the Eddington luminosity of a $3 \times 10^9 M_\odot$ BH. In this regard the BH of in M 87 is similar to the supermassive BH in the center of our galaxy. In both cases the low bolometric luminosity of the nucleus makes the “central engine” of activity, i.e. the vicinity of the event horizon of the supermassive BH, transparent to the very high energy (VHE) γ -rays (Aharonian & Neronov 2005).

In the isotropic field of background photons, the cross-section of photon-photon pair production depends on the product of energies of colliding photons, $s = E\epsilon/m_e^2$. Starting from the threshold at $s = 1$, the cross-section $\sigma_{\gamma\gamma}$ rapidly increases achieving the maximum $\sigma_0 \approx \sigma_T/5 \simeq 1.3 \times 10^{-25}$ cm² at $s \approx 4$, and then decreases as s^{-1} lns. Because of relatively narrow distribution of $\sigma_{\gamma\gamma}(s)$, gamma-rays interact most effectively with the infrared background photons of energy

$$\epsilon \approx 1(E/1 \text{ TeV})^{-1} \text{ eV} . \quad (1)$$

Thus the optical depth for a gamma-ray of energy E produced in the center of the infrared source of the size R_{IR} and the luminosity L_{IR} at energy given by Eq.(1) can be written in the form

$$\tau(E, R_{\text{IR}}) = \frac{L_{\text{IR}}\sigma_{\gamma\gamma}}{4\pi R_{\text{IR}}\epsilon} \simeq \quad (2)$$

$$0.1 \left[\frac{L_{\text{IR}}(1[E/1\text{TeV}]^{-1}\text{eV})}{3 \times 10^{40} \text{ erg/s}} \right] \left[\frac{R_{\text{IR}}}{50R_{\text{Schw}}} \right]^{-1} \left[\frac{E}{1 \text{ TeV}} \right].$$

The dependence of the optical depth on gamma-ray energy is determined by the spectral form of background radiation $n(\epsilon) = L_{\text{IR}}(\epsilon)/(4\pi R\epsilon)$. In particular, in the case of power-law spectrum with photon index Γ ($n(\epsilon) \propto \epsilon^{-\Gamma}$, or $L_{\text{IR}}(\epsilon) \propto \epsilon^{-\Gamma+1}$, one has $\tau(E, R_{\text{IR}}) \propto E^{\Gamma-1}$. Accurate numerical calculations of the optical depth for the spectral energy distribution of the compact infrared source in the nucleus of M87 (see Fig.8, Section 5) and normalized to the source size $R_{\text{IR}} = 50R_{\text{Schw}}$ is shown by black solid curve in the upper panel of Fig.1. Since $\tau(E, R_{\text{IR}}) \propto R_{\text{IR}}^{-1}$, the optical depth does not exceed 1 even at the highest detected energies of gamma-rays of about 10 TeV, provided that infrared source is larger than $50R_{\text{Schw}}$. This is demonstrated in the lower panel of Fig. 1. Note that the recent claim by Cheung et al. (2007) that the central region of M87 is excluded as a site of the TeV emission because of absorption of γ -rays, is misleading. The authors obtained very large optical depth relevant to the energy $\simeq 25$ TeV and assuming an extremely compact infrared source with a linear size of $R = R_{\text{g}} = R_{\text{Schw}}/2$ (the estimate of the optical depth by Cheung et al. (2007) is shown by a cross in the upper panel of Fig. 1, and the dependence of the optical depth on the γ -ray energy is shown by the grey dashed curve). Although formally one cannot rule out such a compact size of the IR source, a significantly larger size cannot be *a priori* excluded either. Moreover, there are not special reasons to assume that the infrared source is located very close to the event horizon.

For the nucleus of M 87, there are no direct measurements of the size of the infrared source. Observations in the microwave band at 43 GHz suggest that the size of the source at the mm wavelength is limited by 5×10^{16} cm, or approximately $50R_{\text{Schw}}$. Lower angular resolution of the infrared telescopes does not allow us to constrain (or marginally resolve, see Perlman et al. (2001)) the size of the nuclear source to ≤ 10 pc (Whysong & Antonucci 2004). However, even assuming that the size of the infrared source is comparable to the size of the microwave source, one finds from the above estimate that the nucleus can be transparent to γ -rays with energies up to ~ 10 TeV.

Even in the case of the "maximally compact" infrared source of the size $R_{\text{IR}} \sim R_{\text{Schw}}/2$, the source is partially transparent for γ -rays. In spite of the fact that the optical depth for γ -rays produced in the center of the infrared source γ -rays becomes very large at energies $E > 10$ TeV (see the dashed grey curve on the upper panel of Fig. 1), there is no catastrophic absorption of multi-TeV γ -rays. The reason is that in this case the source(s) of γ -ray photons are distributed throughout the infrared source and the thickness H of the transparent surface layer of the source is determined from the condition $\tau(E, H) \simeq 1$.

Assuming a homogeneous γ -ray source, one can find that the luminosity of the last transparent layer ($\tau \leq 1$) is only moderately, by a factor of $H/R_{\text{IR}} \sim \tau(E, R_{\text{IR}})$ (rather than by a factor of $\exp(-\tau(E, R_{\text{IR}}))$ lower than the total luminosity of the source. The attenuation of the γ -ray flux in the case of the γ -ray source distributed throughout the infrared source is shown by dashed curves in the lower panel of Fig. 1 for both cases of $50R_{\text{Schw}}$ (black) and $R_{\text{Schw}}/2$ (grey) size of the infrared source. We assume the suppression factor $(1 + \tau(E, R_{\text{IR}}))^{-1}$ which is an interpolation between no suppression in the $\tau = 0$ limit and $1/\tau$ suppression in the $\tau \gg 1$ limit.

The γ -rays after they escape the nucleus are further attenuated due the pair production in the radiation fields both inside and outside the elliptical galaxy M87. The spectrum of emission from the galactic bulge of M 87 sharply peaks at photon energies around $\epsilon_{\text{bulge}} \simeq 1$ eV. Interactions of nuclear γ -rays with the photon background in M 87 galaxy should therefore lead to maximum absorption at γ -ray energies around $E_{\gamma} \simeq 1$ TeV. The column density of infrared/optical photons in the bulge of the size R_{bulge} and luminosity L_{bulge} along the line of sight is estimated as

$$N_{ph}(1 \text{ eV}) = \int_0^{R_{\text{bulge}}} n_{ph}(r) dr \simeq \quad (3)$$

$$5 \times 10^{23} \left[\frac{L_{\text{bulge}}}{10^{45} \text{ erg/s}} \right] \left[\frac{1 \text{ kpc}}{R_{\text{bulge}}} \right] \text{ cm}^{-2},$$

which allows to estimate the optical depth of gamma-rays at 1 TeV:

$$\tau_{\text{M 87}}(1 \text{ TeV}) = \sigma_0 N_{ph}(1 \text{ eV}) \simeq \quad (4)$$

$$0.08 \left[\frac{L_{\text{bulge}}}{10^{45} \text{ erg/s}} \right] \left[\frac{R_{\text{bulge}}}{1 \text{ kpc}} \right]^{-1}$$

Propagation of γ -rays through the cosmic microwave and infrared backgrounds over the way from M 87 to the observer leads to further absorption of the highest energy quanta. Photons with energies above 10^{15} eV are completely absorbed due to interactions with the 2.7 K microwave background (the minimal propagation distance is ~ 8 kpc). Photons with energies above 100 TeV interact most efficiently with the far-infrared background photons whose density is some 3 orders of magnitude lower than the density of the microwave photons. However, the mean free path of $E \geq 10$ TeV γ -rays interacting with far-infrared background, is still shorter than the distance to M 87 (16 Mpc).

3. PHYSICAL PARAMETERS OF THE CENTRAL ENGINE

The high resolution observations of the nucleus of M 87 in X-rays with the *Chandra* observatory provide an important information about the accretion onto the supermassive BH (Di Matteo et al. 2003). In particular, they give an estimate of the electron density of plasma with a temperature $kT \sim 1$ keV,

$$n_e \simeq 0.1 \text{ cm}^{-3} \quad (5)$$

at the distance of the order of Bondi accretion radius, $R_{\text{Bondi}} \simeq 5 \times 10^5 R_{\text{Schw}}$. The corresponding accretion rate inferred from this estimate is

$$\dot{M}_{\text{Bondi}} \simeq 0.1 M_{\odot} \text{ yr}^{-1}. \quad (6)$$

Interestingly, the observed bolometric luminosity of the nucleus of M 87 is 4 orders of magnitude below the expected nuclear luminosity corresponding to this accretion rate

$$L_{\text{Bondi}} \simeq 10^{45} \left[\frac{\eta}{0.1} \right] \left[\frac{\dot{M}_{\text{Bondi}}}{0.1 M_{\odot}/\text{yr}} \right] \text{ erg/s.} \quad (7)$$

where $\eta \sim 0.1$ is the efficiency of conversion of the rest energy of accreting particles into radiation. This indicates that either the accretion proceeds in a radiatively inefficient way, or the actual accretion rate is still lower than the one inferred from X-ray observations.

To estimate the plasma density close to the event horizon of the black hole, one has to assume a certain radial density profile, $n(r) \sim r^{-\gamma}$. Depending on the model of accretion flow, the index γ can vary between 1/2 (this value is, in fact, a lower limit which can be realized for collisionless motions of individual particles in the central gravitational field) and 3/2. The lack of information about the accretion regime leads to a significant uncertainty of the plasma density near the event horizon,

$$10^{1.5} \text{ cm}^{-3} < n < n_{\text{max}} \simeq 10^{6.5} \text{ cm}^{-3}. \quad (8)$$

Regardless of the uncertainty of this estimate, one may conclude that the strength of magnetic field in the vicinity of the BH can not be very high. Indeed, assuming that the magnetic field is generated by the accreting matter, one can find that the energy density of magnetic field can not exceed the density of the total kinetic energy stored in the particles of the accretion flow. In this case even if the accreting matter moves with relativistic speed, the estimate of maximal possible magnetic field is (assuming that the matter density is $n \sim n_{\text{max}}$)

$$B_{\text{eq}} \simeq (8\pi n_{\text{max}} m_e)^{1/2} \sim 10 \text{ G.} \quad (9)$$

Thus, particle acceleration close to the BH horizon proceeds in the relatively low-density and low-magnetic field environment which significantly limits the range of possible mechanisms of VHE γ -ray emission. Even for the maximally possible acceleration rate, $dE/dt \simeq eB_{\text{eq}}$, one can find that particles accelerated in a region of a linear size of about the Schwarzschild radius can not reach energies higher than

$$E_{\text{max}} \leq eB_{\text{eq}} R_{\text{Schw}} \simeq 10^{18} \text{ eV,} \quad (10)$$

unless the magnetic field is significantly larger than the equipartition estimate, given by Eq. (9).

4. GAMMA-RAY EMISSION FROM ACCELERATED PROTONS.

Protons accelerated near the BH horizon can produce γ -ray emission in the VHE band through several radiation mechanisms. For example, TeV emission can be synchrotron or curvature γ -ray emission which accompanies proton acceleration (Levinson 2000; Aharonian et al. 2002; Neronov et al. 2005). The energy loss time for protons emitting synchrotron radiation at the energy $\epsilon_{\text{synch},p}$ is short enough to explain the observed day-scale variability of the signal,

$$t_{\text{synch},p} \simeq 2.5 \left[\frac{B}{10 \text{ G}} \right]^{-3/2} \left[\frac{\epsilon_{\text{synch},p}}{1 \text{ TeV}} \right]^{-1/2} \text{ d,} \quad (11)$$

However, the energy of synchrotron and/or curvature photons produced by protons accelerated to the energy E_{max} , given by Eq. (10) is too low to explain the emission at 1-10 TeV,

$$\epsilon_{\text{synch},p} \simeq 0.1 \left[\frac{B}{10 \text{ G}} \right] \left[\frac{E_p}{10^{18} \text{ eV}} \right]^2 \text{ GeV} \quad (12)$$

and

$$\epsilon_{\text{curv},p} \simeq 0.01 \left[\frac{E_p}{10^{18} \text{ eV}} \right]^3 \left[\frac{R_{\text{Schw}}}{R_{\text{curv}}} \right] \text{ GeV} \quad (13)$$

(assuming that typical curvature radius of proton trajectories is $R_{\text{curv}} \sim R_{\text{Schw}}$). The γ -ray emission from the accelerated protons is thus expected in the 10 MeV - 10 GeV energy region observable by *GLAST*, rather than in the TeV region visible by *HESS*.

It is, in principle, not excluded that during short episodes of enhanced accretion the magnetic field can rise up to 10^3 G , which would, in principle, allow proton acceleration up to the energies $E_{\text{max}} \sim 10^{20} \text{ eV}$. Thus, the energy of curvature emission given by Eq.(13) can extend up to 10 TeV. Note, however, that even in this case the observed emission can not be related to the proton synchrotron radiation which has an intrinsic self-regulated synchrotron cut-off at $\epsilon_{\text{synch}} \leq 0.3 \text{ TeV}$ (Aharonian 2000), if the region of proton acceleration is spatially coincident with the region of synchrotron emission. A potential problem of assumption about transient enhancement (by 4 orders of magnitude, to produce the necessary increase of equipartition magnetic field, see Eq.(9)) of accretion rate is that it should result, in general, in a broad-band flaring activity of the nucleus of M 87, which, however, is not observed.

VHE γ -rays are produced also in proton-proton (*pp*) collisions. However, the interaction time of high-energy protons propagating through the low density medium ($n \leq 10^7 \text{ cm}^{-3}$) is quite large,

$$t_{pp} \simeq \frac{1}{\sigma_{pp} n_{\text{max}}} \simeq 10 \left[\frac{10^7 \text{ cm}^{-3}}{n_{\text{max}}} \right] \text{ yr} \quad (14)$$

($\sigma_{pp} \sim 10^{-26} \text{ cm}^2$ is the proton-proton interaction cross-section). Even if *pp* interactions would significantly contribute to the overall VHE γ -ray emission, they cannot explain the fast day-scale γ -ray flux variability of M 87. Therefore the observed variability should be referred to fast changes in the concentration of multi-TeV protons in the source, i.e. due to adiabatic or escape losses of protons, on timescales comparable to t_{var} . The fast non-radiative losses versus slow rates of γ -ray production at *pp* collisions implies very low efficiency of conversion of the energy of parent protons to the VHE γ -rays, $\kappa = t_{\text{var}}/t_{pp} \leq 3 \times 10^{-4}$. Thus to explain the γ -ray luminosity $L_{\gamma} \sim 3 \times 10^{40} \text{ erg/s}$, the proton acceleration power should exceed $\kappa^{-1} L_{\gamma} \sim 10^{44} \text{ erg/s}$ which is just about the luminosity L_{Bondi} given by Eq. (7), assuming a conventional, 10% or so, efficiency of conversion of the rest mass energy of accreting particles into radiation. (Here we ignore a possible formation of gamma-rays in a relativistic outflow moving towards the observer which in principle would reduce by an order of magnitude this requirement).

The energy requirements to the proton acceleration power can be somewhat relaxed if one invokes interactions of protons with the surrounding radiation fields. Although TeV γ -rays can be produced in a two-step process which includes Bethe-Heitler pair productions ($p\gamma \rightarrow pe^+, e^-$) and synchrotron radiation of secondary electrons, $p\gamma$ interactions become efficient when they proceed through the photomeson production channel. In order to interact with the photons of the infrared source with average energy $\epsilon_{\text{IR}} \sim 10^{-2}$ eV, protons should be accelerated to $E_p \sim [200 \text{ MeV}/\epsilon_{\text{IR}}] m_p \sim 2 \times 10^{19}$ eV. The number density of IR photons in the compact infrared source is

$$n_{\text{IR}} = \frac{L_{\text{IR}}}{4\pi R_{\text{IR}}^2 \epsilon_{\text{IR}}} \simeq \quad (15)$$

$$7 \times 10^9 \left[\frac{L_{\text{IR}}(\epsilon_{\text{IR}})}{10^{41} \text{ erg/s}} \right] \left[\frac{0.01 \text{ eV}}{\epsilon_{\text{IR}}} \right] \left[\frac{50 R_{\text{Schw}}}{R_{\text{IR}}} \right]^2 \text{ cm}^{-3}$$

For the average cross-section of the photo-pion production cross-section, $\sigma_{p\gamma} \sim 10^{-28}$ cm², the interaction time of protons with infrared photons is

$$t_{p\gamma} = \frac{1}{\sigma_{p\gamma} n_{\text{IR}}} \simeq 1.7 \left[\frac{10^{41} \text{ erg/s}}{L_{\text{IR}}(0.01 \text{ eV})} \right] \left[\frac{R_{\text{IR}}}{50 R_{\text{Schw}}} \right]^2 \text{ yr} \quad (16)$$

If the infrared source is very compact, $R_{\text{IR}} \sim R_{\text{Schw}}/2$, and the accretion rate is transiently increased by 2 orders of magnitude (to allow an order-of-magnitude increase in equipartition magnetic field and, as a consequence, proton acceleration to $E > 10^{19}$ eV), the $p\gamma$ cooling time can be as short as the observed TeV variability time scale.

Note that the hypothesis of TeV γ -ray emission of M87 based on the assumption of $p\gamma$ interactions, requires a very compact IR source with a size $R_{\text{IR}} \sim R_{\text{Schw}}$. This implies strong absorption of gamma-rays with fast multiplication of electron-positron pairs via Klein-Nishina cascades. Actually, photon-photon pair production is an important element of any $p\gamma$ model; the observed spectrum of TeV γ -rays cannot be explained by first generation of ultra-high energy ($\geq 10^{15}$) photons from π^0 decays, and therefore requires production of secondary electrons which would provide broad-band emission in the TeV energy band. On the other hand, the copious pair production may lead to neutralization of the large scale ($\geq R_{\text{Schw}}$) electric field, and thus to significant reduction of the maximum achievable energy of protons given by Eq.(10). Since the rate of photomeson processes in the nucleus of M87 is very sensitive to the energy of protons, namely, it requires $E_p \geq 10^{18}$, the generation of large amount of secondary electrons may result in a dramatic drop of the rate of photo-meson production. A non-negligible contribution to the secondary electrons may come also from the Bethe-Heitler pair production, especially when the efficiency of photomeson production is suppressed (the energy threshold of this process is two orders of magnitude smaller than the energy threshold of the photomeson production). Whether this mechanism can explain the observed spectral and temporal characteristics of TeV γ -ray emission from M87, is a question which needs detailed numerical calculations. In any case it is clear that $p\gamma$ models can provide adequate efficiency only in the case of a very compact IR source with a size

close to the Schwarzschild radius.

5. GAMMA-RAY EMISSION FROM ACCELERATED ELECTRONS.

5.1. Order-of-magnitude estimates

The tough requirements of acceleration of protons to ultrahigh energies ($E \geq 10^{18}$ eV), as well as the relevant long cooling times challenge any interpretation of the day-scale variability of TeV γ -rays in terms of interactions of high-energy protons. The models based on acceleration of electrons do not face such problems, and are likely to be responsible for the observed TeV γ -ray emission.

The main emission mechanisms by electrons in the vicinity of the supermassive BH are synchrotron/curvature radiation and inverse Compton (IC) scattering. Electrons can be accelerated to multi-TeV energies only if the strength of the chaotic component of the magnetic field, B_{rand} , in the acceleration region is not too high. Assuming that electrons are accelerated at a rate $dE/dt \sim \kappa e B_{\text{ord}}$ ($\kappa \leq 1$ and B_{ord} is the ordered component of the magnetic field), from the balance of the acceleration and synchrotron energy loss rates one finds

$$E_e \leq \frac{\kappa^{1/2} m_e^2 B_{\text{ord}}^{1/2}}{e^{3/2} B_{\text{rand}}} \simeq \quad (17)$$

$$4 \times 10^{13} \left[\frac{B_{\text{ord}}}{1 \text{ G}} \right]^{1/2} \left[\frac{B_{\text{rand}}}{1 \text{ G}} \right]^{-1} \kappa^{1/2} \text{ eV} .$$

Thus, even in the case of maximum possible acceleration rate ($\kappa = 1$) electrons cannot emit in the 10-100 TeV band unless

$$B_{\text{rand}} \lesssim 1 \text{ G} . \quad (18)$$

In the ordered field the energy dissipation of electrons is reduced to curvature radiation losses. From the balance between the curvature loss rate and the acceleration rate, assuming that the typical curvature radius R_{curv} of magnetic field is comparable to the gravitational radius, one finds

$$E_e = \left[\frac{3m_e^4 R_{\text{curv}}^2 \kappa B_{\text{ord}}}{2e} \right]^{1/4} \simeq \quad (19)$$

$$4 \times 10^{15} \left[\frac{B_{\text{ord}}}{1 \text{ G}} \right]^{1/4} \left[\frac{R_{\text{curv}}}{R_{\text{Schw}}} \right]^{1/2} \kappa^{1/4} \text{ eV} .$$

Thus if the energy losses of electrons are dominated by curvature radiation, the maximum energy of accelerated electrons only weakly depends on the strength of the magnetic field.

The IC loss rate is determined by the energy density of infrared radiation in the nucleus, $U_{ph} = L_{\text{IR}}/(4\pi R_{\text{IR}}^2 c)$. The condition of the balance between IC loss rate and the electron acceleration rate gives

$$E_e \simeq \frac{3^{3/4} m_e^2 B_{\text{ord}}^{1/2} R_{\text{IR}}}{2^{5/4} e^{3/2} L_{\text{IR}}^{1/2}} \simeq \quad (20)$$

$$1 \times 10^{15} \left[\frac{B_{\text{ord}}}{1 \text{ G}} \right]^{1/2} \left[\frac{R_{\text{IR}}}{50 R_{\text{Schw}}} \right] \kappa^{1/2} \text{ eV} .$$

Note that this estimate is obtained assuming that the IC scattering takes place in the Thompson regime. However,

highest energy electrons upscatter the infrared/optical radiation in the Klein-Nishina regime in which the efficiency of the IC scattering is reduced. A proper account of the decrease of the IC loss efficiency would result in higher electron energies exceeding the estimate of Eq. (20).

5.2. Electron acceleration in the vacuum gaps of BH magnetosphere

So far we did not specify the particular mechanism of particle acceleration. In principle, several mechanisms can be responsible for the electron acceleration, but an obvious requirement which follows from the above estimates is that the "efficiency" parameter κ for the acceleration rate should be close to one, otherwise electrons would not reach the ~ 100 TeV energies, as it follows from Eqs. (17),(19),(20). Also, the irregular component of the magnetic field should not exceed 1 G.

Large scale ordered electric fields, induced by rotation of black hole, are known to be responsible for particle acceleration and high-energy radiation in pulsars. A similar mechanism of generation of large electric fields can be realised in the vicinity of a rotating BH placed in an external magnetic field (Wald 1974; Bicak et al. 1976). In the case of pulsars, it is known that the force-free magnetosphere possesses so-called "vacuum gaps" in which the rotation-induced electric field is not neutralized by redistribution of charges. The vacuum gaps work as powerful particle accelerators and sources of pulsed high-energy γ -ray emission. Vacuum gaps with strong rotation-induced electric field can be present also in the vicinity of a rotating black hole (Blandford & Znajek 1977; Beskin et al. 1992). Below we explore whether the observed VHE γ -ray emission from M 87 can be explained by the emission from the vacuum gaps formed in the magnetosphere of the supermassive black hole in M87.

5.2.1. The magnetosphere of rotation-powered black hole

Throughout the magnetosphere the component of electric field directed along the magnetic field lines is neutralized by the charge redistribution, so that a force-free condition $\vec{B} \perp \vec{E}$ is satisfied. The characteristic charge density needed to neutralize the parallel component of electric field in the magnetosphere of a BH rotating with an angular velocity $\vec{\Omega}$ placed in an external magnetic field \vec{B} is the so-called "Goldreich-Julian" density (Goldreich & Julian 1969)

$$n_q \simeq \frac{\vec{\Omega} \cdot \vec{B}_{\text{ord}}}{2\pi e} \simeq \frac{a B_{\text{ord}}}{(GM)^2} \quad (21)$$

($a = \Omega(GM)^2$, the BH rotation moment per unit mass, $0 < a < GM$, is a commonly used parameter of the Kerr metric describing the space-time of rotating black hole; see Appendix).

In general, the charge distribution in the magnetosphere is not static – additional free charges should be continuously supplied throughout the magnetosphere to compensate for the charge loss due to the magnetohydrodynamical outflow. The inefficiency of charge supply can lead to the formation of "gaps" in the magnetosphere in which the parallel component of electric field is not zero and conditions for particle acceleration exist.

In the case of pulsars, there are several potential ways to supply charged particles to the magnetosphere. First of all, the charge can be extracted directly from the surface of the neutron star. Electrons and positrons can be generated also due to pair production in very strong magnetic field. Finally, electron-positron pairs can be created at interactions of γ -rays with low energy photons.

Apart from the extraction of free charges from the surface of the compact object, the same mechanisms can in principle, be responsible for the charge supply to the magnetosphere in the case of black holes. However, in the particular case of the black hole in M87, the pair production of γ -rays in the magnetic field, (a mechanism, assumed e.g. in the Blandford & Znajek (1977) scenario) is not efficient because (1) the magnetic field cannot significantly exceed 10 G and (2) the energy of γ -rays emitted by accelerated particles cannot exceed 100 TeV. On the other hand, the efficiency of the charge supply via the pair production by γ -rays on the soft infrared background depends on the compactness of the infrared source ($\propto L_{\text{IR}}/R$). This process can be efficient only if γ -rays with energies above 10 TeV are present in the compact source.

Since the 10 TeV γ -rays have to be produced by particles accelerated to energies above 10 TeV, the gap(s), in which electric field component along the magnetic field lines is not neutralized by the charge redistribution, should be present in the magnetosphere. In a self-consistent scenario the height of the gap(s) is limited by the condition that γ -rays emitted by the accelerated particles do not produce e^+e^- pairs within the gap.

In order to estimate whether particle acceleration and high-energy emission from the vacuum gaps can be responsible for the observed VHE luminosity of M 87 one has to estimate the total acceleration power output in the gap. In spite of the fact that the potential drop in the gap can be enough to accelerate charge particles to energies as high as 10^{18} eV, strong radiative losses limit the maximum energy of electrons to 10^3 TeV. This means that the propagation of electrons through the gap proceeds in a "loss-saturated" regime: all the work done by the gap's electric field is dissipated through the synchrotron/curvature and/or IC radiation. The rotation induced electric field near the BH horizon has a strength (see Appendix) $\mathcal{E} \sim [a/GM] B_{\text{ord}}$. For each electrons propagating in the gap, the energy loss rate is estimated as $dE/dt \simeq e\mathcal{E} \sim e [a/(GM)] B_{\text{ord}}$.¹ The density of electrons in the gap is limited by the Goldreich-Julian density, given by Eq. (21). If the size of the infrared source is large enough, so that the gap height is not limited by pair production, the size of the gap is estimated to be about $H \sim R_{\text{Schw}}$. Taking into account that the volume of the gap is roughly $R_{\text{Schw}}^2 H$, the total number of electrons in the gap can be estimated as $R_{\text{Schw}}^2 H n_q$. Then the total power output of the gap is

$$P \simeq n_q H R_{\text{Schw}}^2 (dE/dt) \quad (22)$$

$$\sim 5 \times 10^{41} \frac{4a^2}{R_{\text{Schw}}^2} \left[\frac{M}{3 \times 10^9 M_{\odot}} \right]^2 \left[\frac{H}{R_{\text{Schw}}} \right] \left[\frac{B_{\text{ord}}}{10 \text{ G}} \right]^2 \text{ erg/s}$$

¹ This implies that the acceleration efficiency κ is $\kappa \simeq [a/(GM)]$. For the extreme rotating black hole with $a = GM$, the acceleration reaches the maximum possible rate with $\kappa \simeq 1$.

Thus, if the angular momentum of the black hole is large enough, the nonthermal power of the vacuum gap can be as large as the observed TeV gamma-ray luminosity.

5.2.2. Numerical modelling of acceleration and radiation of electrons in the gap of the black hole magnetosphere

Location of the gaps in the BH magnetosphere depends on the structure of both the accretion flow and the magnetic field near the event horizon. In this regard, it should be noted that even after four decades of intensive theoretical study of physics of pulsar magnetospheres, the details of the geometry of vacuum gaps remain uncertain. Nevertheless, the basic properties of particle accelerators operating in the vacuum gaps can be understood with a reasonable accuracy and confidence.

We have developed a numerical code which allows, for the given geometry of the gap and configuration of the magnetic field, a quantitative study of energy distributions of electrons accelerated in the vacuum gap and associated electromagnetic radiation. For demonstration of the importance of the VHE γ -ray emission from the vacuum gaps, in this paper we have chosen a simple geometry of the gap, namely we assumed that the gap occupies a spherical layer above the BH horizon and has the height of about the size of the event horizon. The geometry of electromagnetic field is assumed to be given by the solution of Maxwellian equations in Kerr metric, which corresponds to an asymptotically constant magnetic field inclined at an angle χ with respect to the rotation axis of the black hole (Bicak et al. 1976). The analytical solution of Maxwellian equations are given in Appendix. The initial locations of electrons are assumed to be homogeneously distributed either throughout the gap or over the boundary of the gap. The initial energies of electrons are assumed to be equal to the rest energy. Trajectories have been numerically integrated taking into account effects of General Relativity and energy losses of electrons due to synchrotron/curvature radiation and inverse Compton scattering (see Appendix for technical details). The spectra and angular distributions of the synchrotron and curvature radiation are calculated by tracing the photon trajectories through the Kerr space-time metric from the emission point to infinity.

As an example of numerical modelling, in Fig. 2 we show distributions of average energies of electrons propagating in the spherical layer occupied by the gap. The magnetic field is assumed to be inclined at an angle $\chi = 20^\circ$ with respect to the rotation axis. The two left panels show angular distributions of the average energy of individual electrons and the power of synchrotron/curvature emission, as measured in the Zero Angular Momentum Observer (ZAMO) frame (Bardeen et al. 1972), close to the black hole horizon (see Appendix for details). One can see that the maximum energies of photons are achieved in two oppositely situated hot-spots determined by the direction of magnetic field. At the same time, the total power of radiation does not strongly depend on the latitude and longitude coordinates.

The "dark strips" (one along the equatorial plane and two snake-like dark strips above and below the equatorial plane) are clearly recognizable in the left panels of Fig. 2. The drop of energies is explained by the specific configuration of electromagnetic field in these regions.

Namely, the dark strips surround the so-called "force-free" surfaces at which the rotation-induced electric field \vec{E} is orthogonal to the magnetic field \vec{B}_{ord} .

The right panel of Fig. 2 shows the angular distribution of average photon energies and emissivity after the photon tracing to infinity through the Kerr space-time metric. One can see that polar "hot spots" become more pronounced, mostly because the photons emitted from equatorial regions (from the ergosphere) have larger redshifts and a significant fraction of these photons is just absorbed by the black hole.

Fig. 3 shows evolution of the shape of the polar hot spots with an increase of the inclination angle of the magnetic field. One can see that the shape of the hot spots becomes wider and irregular. Also, with an increase of the inclination of the magnetic field the average photon energy decreases, which is explained by the fact that the acceleration of electrons is most efficient when the electric field is aligned with the magnetic field. With the increase of the magnetic field inclination angle χ , the regions of aligned electric and magnetic field (situated close to the rotation axis of the BH in the case $\chi = 0^\circ$) disappear.

In Fig. 4 a typical spectrum of electrons accelerated in the spherical vacuum gap close to the BH horizon is shown. It is assumed that an extreme rotating BH ($a = GM$) is placed in 1 G magnetic field inclined at an angle of 60° with respect to the rotation axis. The size of the infrared emission region is assumed $R_{\text{IR}} = 10R_{\text{Schw}}$. The three energy spectra shown in Fig. 4 correspond to different strengths of the random component of magnetic field. If the random magnetic field is smaller than 10^{-3} fraction of the ordered field, electrons propagating in the gap reach energies up to $\sim 10^{16}$ eV. With an increase of the random component of magnetic field, the synchrotron losses start to dominate which leads to reduction of the maximum electron energies, in a good agreement with the qualitative estimates of Section 5.1.

5.3. Direct synchrotron/curvature and IC radiation from the acceleration process

The radiative losses through both synchrotron/curvature and IC channels are released in the form of high energy γ -rays. The energy of Compton upscattered photons (in Thompson regime) is

$$\epsilon_{\text{IC}} = 0.4 \left[\frac{\epsilon_{\text{IR}}}{10^{-2} \text{eV}} \right] \left[\frac{E_e}{1 \text{ TeV}} \right]^2 \text{ TeV} \quad (23)$$

The IC scattering of $E_e \gtrsim 10$ TeV electrons on IR photons proceeds in the Klein-Nishina regime, thus $\epsilon_{\text{IC}} \simeq E_e$. The curvature radiation peaks at significantly lower energies,

$$\epsilon_{\text{curv}} = \frac{3E_e^3}{2m_e^3 R_{\text{curv}}} \simeq 0.2 \left[\frac{E_e}{10^{15} \text{ eV}} \right]^3 \left[\frac{R_{\text{Schw}}}{R_{\text{curv}}} \right] \text{ GeV} . \quad (24)$$

Since electron acceleration in the gap proceeds in the "loss saturated" regime, the calculations of the spectral and angular distributions of radiation accompanying the acceleration process, requires "self-consistent" approach in which the spectrum of radiation is calculated simultaneously with the spectrum of parent electrons. The algorithm of self-consistent calculations used in this work

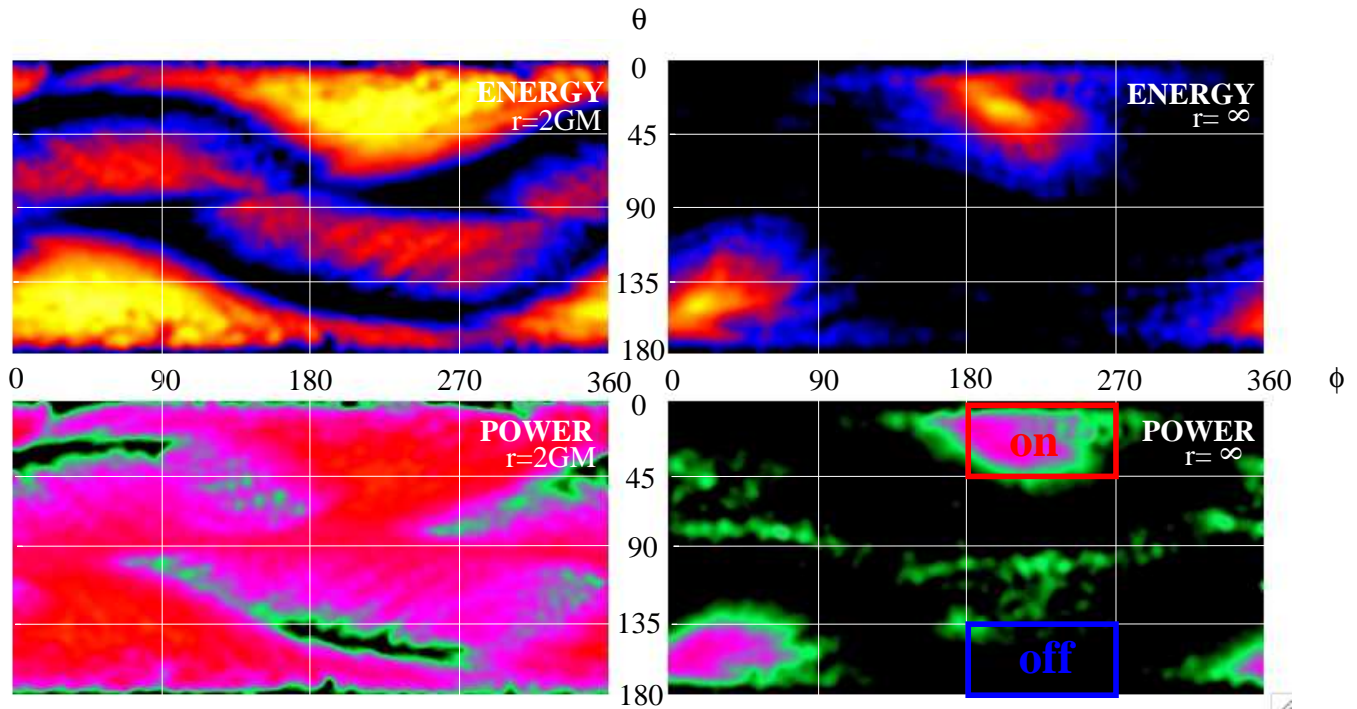


FIG. 2.— Angular distributions of synchrotron/curvature photon energies (top) and γ -ray production rate (bottom) for emission from a spherical vacuum gap close to an extreme rotating BH placed in a magnetic field $B = 1$ G inclined at an angle $\chi = 20^\circ$ with respect to the BH rotation axis. Two left panels show the angular distributions as seen in ZAMO frame close to the black hole horizon. Two right panels show the angular distributions after photon tracing to infinity. The scales are logarithmic and cover two decades from maximum (yellow on the top panels, red on the bottom panels) scale, max , down to the $0.01max$ (black). Red and blue boxes on the bottom right panel show the regions used to extract spectra seen from "on hot spot" and "off hot spot" directions as shown in Fig. 5.

is briefly described in the Appendix.

Some results of self-consistent calculations of the γ -ray production spectra as functions of the viewing angle and the inclination of the magnetic field are shown in Figs. 5 and 6, respectively. Fig. 5 demonstrates the difference of production spectra of γ -rays emitted along the direction of magnetic field (the region marked "on" in Fig. 2) and away from this direction (the region marked "off" in Fig. 2). Fig. 6 demonstrates the dependence of the γ -ray production spectra on the inclination angle of magnetic field. In both figures the low-energy (MeV-GeV) peak is due to the synchrotron/curvature radiation, while the high energy (TeV-PeV) peak is formed due to the IC scattering in the Klein-Nishina regime.

5.4. Isotropic TeV emission from secondary pair-produced electrons

The spectral energy distributions shown in Figs. 5 and 6 correspond to the production rates of the first generation γ -rays. They have essentially anisotropic distribution, thus the calculations of fluxes detected by an observer contain large uncertainties, mainly because of the poor knowledge of the source geometry. However, due to the internal and external absorption of ≥ 10 TeV γ -rays, the observer detects only a tiny fraction of the first generation γ -rays. While interactions with external photon fields lead to real attenuation of the γ -ray flux, the internal absorption is essentially recovered due to radiation of the pair produced electrons of second and further generations. Interestingly, the development of an electromagnetic cascade in radiation field of the infrared source may lead to "isotropisation" of

the γ -ray source. Indeed, the absorption of first generation γ -rays leads to deposition of e^+e^- pairs throughout the infrared source volume, R_{IR} . If the latter is significantly larger than the volume corresponding to the vacuum gap (i.e. $R_{IR} \gg R_{Schw}$), the magnetic field in the IR source can be dominated by the irregular component which would effectively isotropise the directions of secondary electrons. Correspondingly, the secondary radiation from e^+e^- pairs will be emitted isotropically. For any reasonable magnetic field, the synchrotron radiation of secondary electrons is produced at energies significantly below 1 TeV. Therefore for explanation of the observed TeV gamma-radiation one should assume that the energy losses of electrons are dominated by IC scattering, i.e. the magnetic field in the infrared source should be significantly less than $B = (L_{IR}/2R_{IR}^2)^{1/2} \sim 0.1$ G. If so, the absorption of first generation gamma-rays will trigger an electromagnetic (Klein-Nishina) cascade.

In Fig. 7 we show the resulting spectrum of gamma-radiation expected from the internal absorption of first generation gamma-rays. It consists of the isotropic component associated with the cascade in the infrared source (green dashed curve) and the primary anisotropic component whose intensity is uncertain since it strongly depends on the orientation of the observer with respect to the magnetic field direction. In Fig. 7 the thin solid red line corresponds to the sum of these two components, while the thick red solid line shows the result of absorption of the summary spectrum in the infrared source, in the elliptical galaxy M87 and in the intergalactic medium (see thick solid curve in Fig. 1). The curve

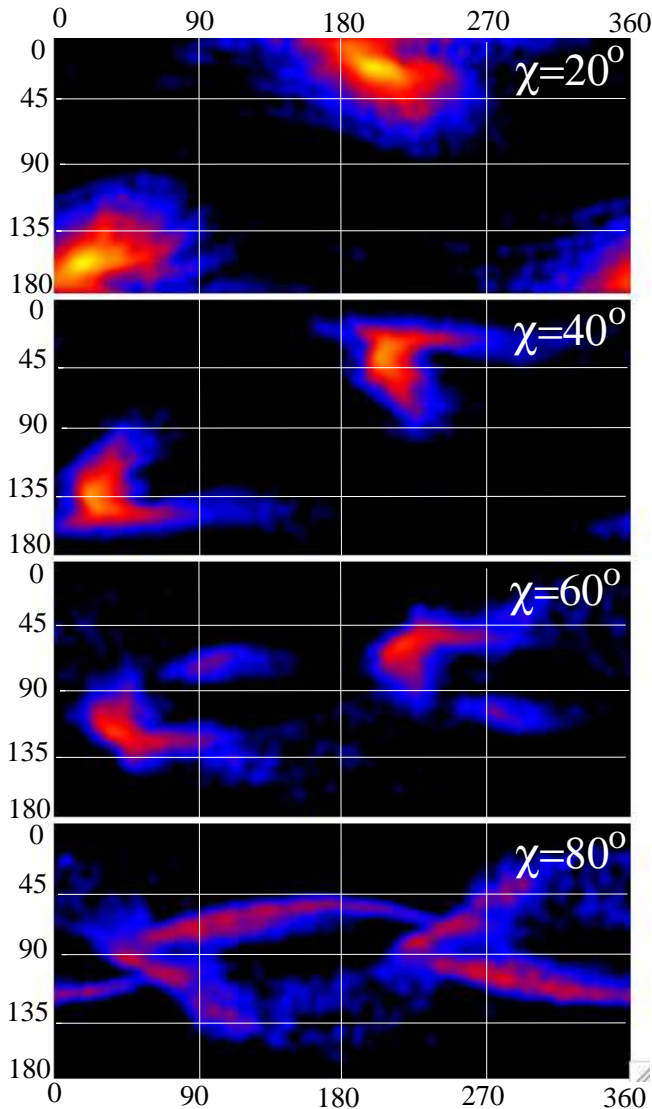


FIG. 3.— Evolution of the shape of the polar hot spots with an increase of the inclination angle of magnetic field. The figures show the angular distribution of the energies of photons of synchrotron/curvature radiation traced to infinity. The color scale and parameters of numerical simulations are the same as in the top right panel of Fig. 2: maximum yellow corresponds to photon energies 10 GeV, minimum (black) to photon energies below 0.1 GeV.

is normalized to the observed flux of γ -rays at 0.5 TeV. The comparison of the calculated γ -ray spectrum shows quite a good agreement with the HESS measurements up to $E \sim 10 - 20$ TeV. One should note, however, that the agreement with the observations should not be over-emphasized, since we consider a "toy model" aimed to demonstrate the importance of TeV emission from the vacuum gaps in the magnetosphere.

Finally in Fig. 8 we show the broad-band spectral energy distribution (SED) of the resulting radiation and compare the model curve with observed fluxes of the nucleus of M87 at infrared, X-ray and TeV gamma-rays. Two broad peaks in the SED correspond to synchrotron radiation and inverse Compton scattering of secondary (cascade) electrons in the infrared source. The condition that the synchrotron emission from the infrared source

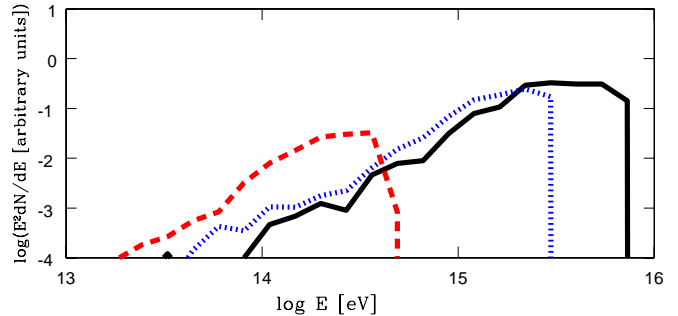


FIG. 4.— Spectrum of electrons accelerated in the vacuum gap above the horizon of a maximally rotating BH of a mass $M = 3 \times 10^9 M_\odot$ placed in an ordered magnetic field $B = 1$ G inclined at $\theta = 60^\circ$ with respect to the BH rotation axis. Black solid line: the random magnetic field is 0.1% of the ordered one; blue dotted line: the random magnetic field is 1%; red dashed line: random magnetic field is 10%.

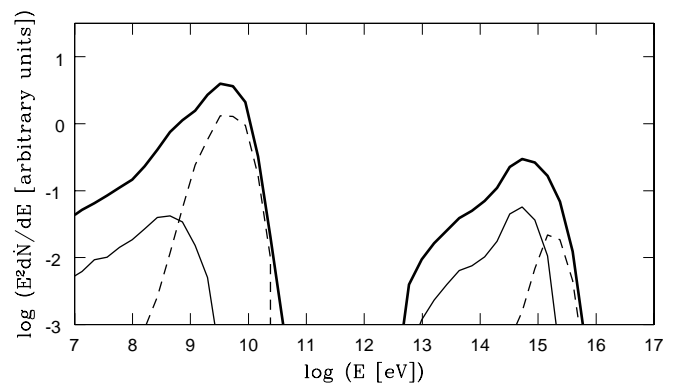


FIG. 5.— The production rate of first generation gamma-rays emitted by the spherical vacuum gap. The physical parameters are the same as in Fig. 2. Thick solid line: the total spectrum integrated over all directions. Dashed line: the spectrum integrated around the "hot spot" (the box marked "on" in Fig. 2). Thin solid line: the spectrum collected from the box marked "off" in Fig. 2.

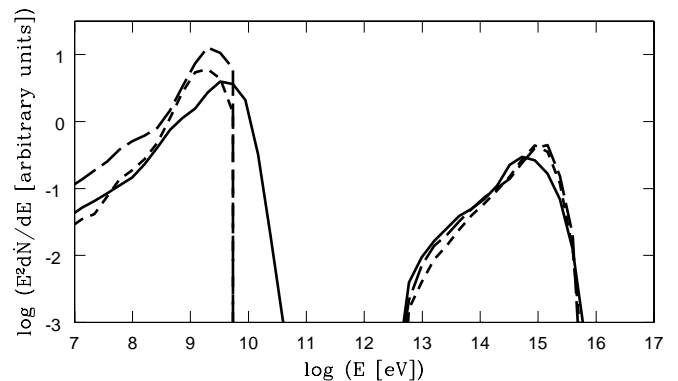


FIG. 6.— The production rates of gamma-rays calculated for different values of the inclination angle of magnetic field. Solid line: $\chi = 20^\circ$; dashed line: $\chi = 60^\circ$; long-dashed line: $\chi = 90^\circ$. Physical parameters are same as in Fig. 2.

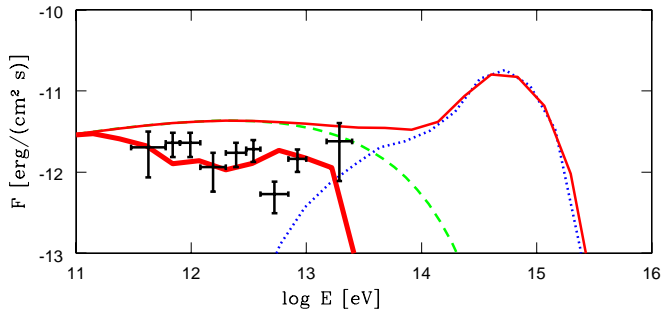


FIG. 7.— Secondary emission from high-energy electrons injected into the compact infrared source in the nucleus of M 87 via the photon-photon pair production. Thick black solid line: omnidirectional spectrum of primary emission from accelerated particles; thin blue solid line: the primary spectrum only from the "off" direction (same as in Fig. 5); black and blue thin dashed lines show the spectra attenuated by the pair production in the infrared source. Red dotted line shows the contribution of secondary cascade (isotropic) emission.

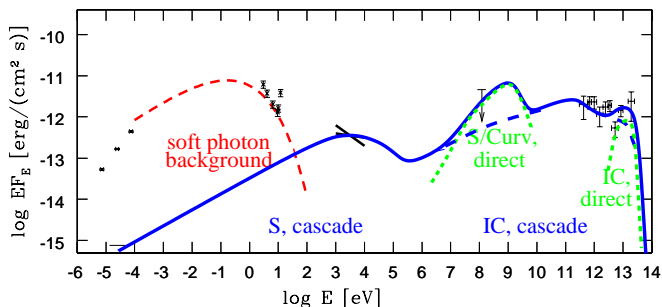


FIG. 8.— Spectral energy distribution of emission from the nucleus of M 87. Dashed blue line: isotropic synchrotron and IC emission from secondary electron-positron pairs injected via the pair production. Short-dashed green line: direct synchrotron/curvature and IC emission from electrons accelerated in the vacuum gap (strongly anisotropic, depends on the geometry of the vacuum gap). Solid blue line shows the total emission spectrum, which is the sum of the direct and cascade contributions. Dashed red line shows the model spectrum of soft photon background used for the calculation of IC scattering. This radiation component can come from a larger region and is not necessarily related to the particle acceleration in the vacuum gap.

should not exceed the observed flux in the X-ray band imposes an upper limit on the random magnetic field strength $B < 0.1(R_{IR}/R_{Schw})^{-1}$ G. The existing upper limit on the M87 flux in the EGRET energy band (Sreekumar et al. 1994) imposes a restriction on the direct synchrotron/curvature emission from gap emitted in the direction of observer.

Because of uncertainties of model parameters as well as the strong variability of radiation, we do not attempt to make a detailed fit to the broad band spectrum of the source, especially taking into account that the measurements at different energy bands correspond different epochs. On the other hand, the future simultaneous studies of temporal and spectral properties of the broad-band emission can provide meaningful tests of the proposed model and significantly reduce the relevant parameter space.

6. SUMMARY AND CONCLUSIONS.

We have studied the mechanisms of production of variable TeV γ -ray emission from vicinity of the supermas-

sive BH in the nucleus of M 87. Moderate accretion rate onto the black hole, inferred from the *Chandra* observations, limits the magnetic field strength close to the black hole horizon - it cannot significantly exceed $B \leq 10$ G. This limits the maximum energy attainable by protons, $E \leq 10^{18}$ eV. None of the known mechanisms of γ -ray emission by protons can satisfactorily explain the observed temporal and spectral characteristics of the observed TeV γ -ray emission. On the other hand, severe radiative losses of electrons in a compact region close to the black hole significantly constrains the range of possible acceleration scenarios. In particular the random component of the magnetic field cannot exceed 1 G. Thus, the acceleration takes place, most likely, in a region where the regular magnetic field significantly exceeds the random component of the field. Even so, the unavoidable energy losses due to the curvature radiation and inverse Compton scattering require an extremely effective mechanism of particle acceleration with a rate close to the maximum (theoretically possible) acceleration rate.

In this paper we show that the observed TeV gamma-ray emission from M87 can be explained by electrons accelerated in strong rotation induced electric fields in the vacuum gaps in black hole magnetosphere. Generally, this model has many similarities with models of particle acceleration in pulsar magnetospheres. Our detailed modelling shows that the gamma-radiation from the central engine of M 87 consists of both first generation photons emitted by particles accelerated in the gap (severely attenuated due to interactions with the internal and external radiation fields) and second and further generation (cascade) photons. If the first component dominates above 10 TeV, the cascade γ -rays contribute mainly to the ≤ 10 TeV energy domain. The electron acceleration and γ -ray production in a very compact region close to the event horizon of the black hole naturally explains the observed variability of TeV γ -ray emission from M87.

7. ACKNOWLEDGEMENT.

We would like to thank V.Beskin for the clarifying comments on the manuscript.

APPENDIX

DETAILS OF THE NUMERICAL MODELLING OF PARTICLE ACCELERATION IN THE VACUUM GAPS IN MAGNETOSPHERES OF ROTATING BLACK HOLE.

A self-consistent modelling of acceleration of electrons in the direct vicinity of event horizon of a BH requires (a) a full account of the effects of General Relativity and (b) a full account of the radiation reaction on particle motion, since electrons propagate most of the time in the "loss saturated" regime when the acceleration force is balanced by the radiation reaction force. Below we give some details of the modelling of trajectories electrons and photons in the vicinity of the black hole.

The Kerr space-time.

A rotating BH is described by two parameters: its mass M and the angular momentum per unit mass $a \leq GM$. The geometry of space-time in the vicinity of horizon is described by the Kerr metric

$$ds^2 = -\alpha^2 dt^2 + g_{ik} [dx^i + \beta^i dt] [dx^k + \beta^k dt] \quad (\text{A1})$$

$$\alpha = \frac{\rho\sqrt{\Delta}}{\Sigma}; \quad g_{rr} = \frac{\rho^2}{\Delta}; \quad g_{\theta\theta} = \rho^2; \quad g_{\phi\phi} = \frac{\Sigma^2 \sin^2 \theta}{\rho^2};$$

$$\beta_\phi = -\frac{2aGMr}{\Sigma^2}; \quad \Delta = r^2 + a^2 - 2GMr;$$

$$\Sigma^2 = (r^2 + a^2)^2 - a^2 \Delta \sin^2 \theta; \quad \rho^2 = r^2 + a^2 \cos^2 \theta \quad (\text{A2})$$

The horizon is situated at $r_H = GM + \sqrt{(GM)^2 - a^2}$.

To understand the acceleration and energy losses of charged particles propagating close to the BH horizon, it is convenient to use an orthonormal (non-coordinate) frame

$$e_{\hat{t}} = \frac{\Sigma}{\rho\sqrt{\Delta}} \frac{\partial}{\partial t} + \frac{2GMa r}{\Sigma\rho\sqrt{\Delta}} \frac{\partial}{\partial \phi}; \quad e_{\hat{r}} = \frac{\sqrt{\Delta}}{\rho} \frac{\partial}{\partial r}; \quad e_{\hat{\theta}} = \frac{1}{\rho} \frac{\partial}{\partial \theta}; \quad e_{\hat{\phi}} = \frac{\rho}{\Sigma \sin \theta} \frac{\partial}{\partial \phi}. \quad (\text{A3})$$

carried by the so-called "zero angular momentum" observers (ZAMO) (Bardeen et al. 1972). The corresponding covariant basis vectors $e^{\hat{i}}$ are given by

$$e^{\hat{t}} = \frac{\rho\sqrt{\Delta}}{\Sigma} dt; \quad e^{\hat{r}} = \frac{\rho}{\sqrt{\Delta}} dr; \quad e^{\hat{\theta}} = \rho d\theta, \quad e^{\hat{\phi}} = \frac{\Sigma \sin \theta}{\rho} d\phi - \frac{2GMa r \sin \theta}{\rho\Sigma} dt. \quad (\text{A4})$$

The electromagnetic field.

In the reference frame (A3) the magnetic field inclined at angle χ with respect to the BH rotation axis is given by (Bicak et al. 1976)

$$\begin{aligned} B^{\hat{r}} &= \frac{1}{\Sigma\rho^4 \sin \theta} \{ B_{\parallel} \sin \theta \cos \theta [\Delta\rho^4 + 2GMr(r^4 - a^4)] + \\ &\quad B_{\perp} [r \cos \psi - a \sin \psi] [\rho^4(r \sin^2 \theta + GM \cos 2\theta) - \\ &\quad GM(r^2 + a^2)(r^2 \cos 2\theta + a^2 \cos^2 \theta)] \} \\ B^{\hat{\theta}} &= -\frac{1}{\Sigma\rho^4 \sqrt{\Delta}} \{ B_{\parallel} \Delta \sin \theta [\rho^4 r + a^2 GM(r^2 - a^2 \cos^2 \theta)(1 + \cos^2 \theta)] + \\ &\quad B_{\perp} \cos \theta [\rho^4 ((\Delta r - GMa^2) \cos \psi + a(\Delta + GMr) \sin \psi) - \\ &\quad a^2 GMr \sin^2 \theta (r^2(r - 2GM) + 2a^2(r \sin^2 \theta + GM \cos^2 \theta)) \cos \psi - \\ &\quad a(\Delta - 2GMr - 2a^2 \cos^2 \theta) \sin \psi] \} \end{aligned} \quad (\text{A5})$$

where

$$\psi = \phi + \frac{a}{2\sqrt{(GM)^2 - a^2}} \ln \left[\frac{r - GM + \sqrt{(GM)^2 - a^2}}{r - GM - \sqrt{(GM)^2 - a^2}} \right]; \quad B_{\parallel} = B_0 \cos \chi, \quad B_{\perp} = B_0 \sin \chi. \quad (\text{A6})$$

Rotation of the BH is responsible for the appearance of nonzero electric field whose components are

$$\begin{aligned} E^{\hat{r}} &= \frac{aGM}{\Sigma\Delta\rho^6} \{ B_{\parallel} \Delta [2r^2\rho^4 \sin^2 \theta - (\Sigma^2 - 2GMra^2 \sin^2 \theta)(r^2 - a^2 \cos^2 \theta)(1 + \cos^2 \theta)] - \\ &\quad B_{\perp} r \sin \theta \cos \theta [2 [(r\Delta - GMa^2) \cos \psi - a(\Delta + rGM) \sin \psi] + \\ &\quad (\Sigma^2 - 2GMra^2 \sin^2 \theta) [r^2(r - 2GM) + 2a^2(r \sin^2 \theta + GM \cos^2 \theta) \cos \psi - \end{aligned}$$

$$E^{\hat{\theta}} = \frac{aGM}{\Sigma\sqrt{\Delta}\rho^6} \left\{ 2B_{\parallel} r \sin\theta \cos\theta [\Delta\rho^4 - (r^2 - a^2) [\Sigma^2 - 2GMr(r^2 + a^2)]] + \right. \\ \left. B_{\perp} [2r\rho^4 [r(r\sin^2\theta + GM\cos 2\theta)\cos\psi - a(r\sin^2\theta + GM\cos^2\theta)\sin\psi] - \right. \\ \left. (r^2\cos 2\theta + a^2\cos^2\theta) [\Sigma^2 - 2GMr(r^2 + a^2)] (a\sin\psi - r\cos\psi) \right\} \quad (\text{A7})$$

Equations of motion for a charged particle.

The components of the four-velocity of a particle $v^{\mu} = dx^{\mu}/dt$ in the orthonormal frame $e_{\hat{a}}$ (A4) are

$$v^{\mu} = v^{\hat{a}} e_{\hat{a}}^{\mu} d\hat{t}/dt \quad (\text{A8})$$

where \hat{t} is the time which would be locally by the ZAMO observers at a given point and t is the coordinate time which enters the metric (A1). For example, the ϕ components of particle velocity in coordinate and orthonormal reference frame are related through

$$v^{\hat{\phi}} = \frac{\Sigma \sin\theta}{\rho} \left[\frac{d\phi}{dt} - \frac{2GMa r}{\Sigma^2} \right] \frac{dt}{d\hat{t}} \quad (\text{A9})$$

The extra term $\Omega = 2GMa r/\Sigma^2$ is the angular velocity of the ZAMO frame at each point. From (A4) one can see that

$$\frac{d\hat{t}}{dt} = \frac{\rho\sqrt{\Delta}}{\Sigma} \quad (\text{A10})$$

It is convenient to introduce a particle γ -factor in the orthonormal frame $\gamma = 1/\sqrt{1 - (v^{\hat{a}})^2}$.

Equations of motion in the orthonormal basis (A3) have the same form as in the flat space (Thorne et al. 1986)

$$\frac{d\vec{p}}{d\hat{t}} = e(\vec{E} + \vec{v} \times \vec{B}) + m\gamma\vec{g} + \hat{H}\vec{p} + \vec{f}_{rad} \quad (\text{A11})$$

where \vec{p} is the particle momentum

$$p^{\hat{a}} = m\gamma v^{\hat{a}} \quad (\text{A12})$$

\vec{g} is the gravitational acceleration and \hat{H} is the tensor of gravi-magnetic force. The force \vec{f}_{rad} is the radiation reaction force. In the case of interest the time scales for acceleration in electromagnetic field and of the radiation reaction are orders of magnitude shorter than that of the motion of the particle in the gravitational field of the black hole.

The radiation reaction force \vec{f}_{rad} for the ultra-relativistic particles moving in external electromagnetic field is (see, e.g. (Landau & Lifshitz 1975))

$$\vec{f}_{rad} = \frac{2e^4\gamma^2}{3m^2} \left[(\vec{E} + \vec{v} \times \vec{B})^2 - (\vec{v} \cdot (\vec{E} + \vec{v} \times \vec{B}))^2 \right] \frac{\vec{v}}{|\vec{v}|} \quad (\text{A13})$$

Note that if particles move at large angle with respect to the magnetic field lines, this expression will describe mostly synchrotron energy loss. However, in the case when particles move almost along the magnetic field lines, the last equation will "mimic" the effect of curvature energy loss (taking into account the fact that the typical curvature radius of the magnetic field lines in the considered case is about R_{Schw}).

REFERENCES

- Aharonian, F.A., 2000, *New AR*, 5, 377.
 Aharonian F.A. and Neronov, A. 2006, *Ap.J.*, 619, 306
 Aharonian, F. A., Belyanin, A. A., Derishev, E. V., Kocharovskiy, V. V., Kocharovskiy, V.I. V. 2002, *Phys Rev. D*, 66, id. 023005
 Aharonian, F. et al. (HEGRA collaboration) 2003, *A&A*, 403, L1
 Aharonian, F. et al. (HESS collaboration) 2006, *Science*, 314, 1424
 Bardeen, J.M., Press, W.H., Teukolsky, S.A., 1972, *Ap.J.* 178, 347.
 Beskin V.S., Istomin Ya.N., Par'ev V.I., 1992, *Soviet Astronomy*, 36, 642.
 Bicak J., Dvorak L., 1976, *Gen.Rel.Grav.*, 7, 959; see also Bicak J., Janis V., 1985, *MNRAS*, 212, 899.
 Biretta, J. A., Sparks, W. B., & Macchetto, F., 1999, *ApJ*, 520, 621.
 Blandford R.D., Znajek R.L., 1977, *MNRAS*, 179, 433.
 Cheng K.S., Ho C., Ruderman M., 1986, *Ap.J.* 300, 500.
 Cheung C.C., Harris D.E., Stawarz L., 2007, *Ap.J.Lett.* accepted, arXiv:0705.2448.
 Di Matteo T., Allen S.W., Fabian A.C., Wilson A.S. Young A.J. 2003, *ApJ*, 582, 133.
 Fabian, A. 2006, *Science*, 314, 1398
 Georganopoulos, M., Perlman, E. S., Kazanas, D. 2005, *ApJ*, 634, L33
 Goldreich P., Julian W.H., 1969, *Ap.J.* 157, 869.
 Harris D.E., Biretta A.J., Junor W., Perlman E.S., Sparks W.B., Wilson A.S., 2003, *Ap.J.*, 586, L41.
 Heinz S.; Begelman M.C., 1997, *Ap.J.*, 490, 653
 Landau L.D., Lifshitz, E.M., 1975 *The Classical Theory of Fields*, Oxford: Pergamon Press
 Levinson A., 2000, *Phys. Rev. Lett.*, 85, 912.
 Marconi, A., Axon, D. J., Macchetto, F. D., Cappetti, A., Sparks, W. B., Crane, P. 1997, *MNRAS*, 289, L21
 Michel F.C., 2004, *Ad.Sp.R.*, 33, 542.
 Neronov A., Semikoz D., Aharonian F., Kalashev O., 2002, *Phys.Rev. Lett.*, 89, 1101.
 Neronov A., Tinyakov P., Tkachev I., 2005, *JETP*, 100, 656.
 Perlman E.S., Sparks W.B., Radomski J., Packham C., Fisher R.S., Pina R., Biretta J.A. 2001, *Ap.J.*, 561, L51.
 Reimer, A., Protheroe, R. J., Donea, A.-C. 2004, *A&A*, 419, 89
 Sreekumar P. et al., 1994, *Ap.J.* 426, 105.

Stawarz, L., Siemiginowska, A., Ostrowski, M., Sikora, M. 2005
Ap.J., 626, 120
Stawarz, L., Aharonian, F., Kataoka, J., Ostrowski, M.,
Siemiginowska, A., Sikora, M. 2006, MNRAS, 370, 981
Thorne K.S., Price R.H, Macdonald D.A., 1986, *Black Holes: the
Membrane Paradigm*, Yale University Press.

Tonry, J. L. 1991, ApJ, 373, L1
Wald R.M., 1974, Phys.Rev., D10, 1680.
Whysong D., Antonucci R., 2004, Ap.J., 602, 16.
Young A.J., Wilson A.S., Mundell C.G., 2002, Ap.J., 579, 560.